Prostate International 10 (2022) 108–116

Contents lists available at ScienceDirect

Prostate International

journal homepage: https://www.journals.elsevier.com/prostate-international

Original Article

Diagnostic value of integrated ^{18}F-PSMA-1007 PET/MRI compared with that of biparametric MRI for the detection of prostate cancer

Yuping Zeng [a,b,c], Xiaoming Leng [c], Hengbin Liao [c], Guihua Jiang [b,a,*], Ping Chen [c,**]

[a] The Second School of Clinical Medicine, Southern Medical University, Guangzhou 510317, China
[b] Department of Medical Imaging, Guangdong Second Provincial General Hospital, Guangzhou 510317, China
[c] Guangzhou Universal Medical Imaging Diagnostic Center, Guangzhou 510080, China

ARTICLE INFO

Article history:
Received 9 January 2022
Received in revised form
9 March 2022
Accepted 22 March 2022
Available online 28 March 2022

Keywords:
^{18}F-PSMA-1007
PET/MRI
bpMRI
Prostate cancer
Diagnostic value

ABSTRACT

Objective: To assess the diagnostic value of fluorine 18 (^{18}F)-labeled prostate-specific membrane antigen (PSMA)-1007 Positron emission tomography/Magnetic resonance imaging (PET/MRI) and compared with that of biparametric MRI (bpMRI) for the detection of prostate cancer (PCa).

Materials and methods: The study enrolled 29 patients with suspected PCa preoperatively who underwent ^{18}F-PSMA-1007 PET/MRI and subsequent targeted biopsy for suspected PCa lesions. Two readers independently assessed the images of each suspected PCa lesion and determined their overall assessment category on bpMRI and ^{18}F-PSMA-1007 PET/MRI. By using biopsy histopathology as the reference standard, the accuracies of ^{18}F-PSMA-1007 PET/MRI and bpMRI for the detection of PCa lesion were determined. Furthermore, the receiver-operating characteristic (ROC) curves of their semi-quantitative parameters of the optimal standardized uptake value (SUVmax) and apparent diffusion coefficient (ADC) for detecting PCa lesions were derived, and their correlations with the International Society of Urological Pathology (ISUP) grade were reported.

Results: Of the 48 suspected PCa lesions in 29 patients, 38 were pathologically diagnosed with clinically significant PCa and 10 with nonprostate cancer (non-PCa) lesions. Compared with the pathological results, ^{18}F-PSMA-1007 PET/MRI demonstrated much greater diagnostic accuracy (area under the curve, AUC), sensitivity, specificity, positive predictive value, and negative predictive value than bpMRI: 0.974 versus 0.711, 94.74% versus 92.11%, 100% versus 50%, 100% versus 87.50%, and 83.33% versus 62.50%, respectively. The semi-quantitative parameters of SUVmax demonstrated a higher AUC of 0.874 than that of ADC with 0.776 for detecting PCa. The ISUP grade was positively associated with SUVmax at spearman's rho correlation coefficient (Rho) = 0.539, p = 0), but not associated with ADC (Rho = −0.105, p = 0.529).

Conclusion: The diagnostic value of ^{18}F-PSMA-1007 PET/MRI for the detection of PCa is better than that of bpMRI, and a high SUVmax may indicate a lesion with a high ISUP grade.

1. Introduction

Prostate cancer (PCa) is a common malignant tumor of the genitourinary system in older men.[1] With the aging of our society, its incidence and mortality rate are increasing and require our attention.[2] Since there are no obvious clinical symptoms of PCa, the best time window for treatment may be missed after patients are diagnosed.[3] Imaging diagnosis is of necessity for patients to win

Abbreviations: ADC, Apparent diffusion coefficient; AUC, Area under the curve; bpMRI, Biparametric MRI; CI, Confidence interval; DCE, Dynamic contrast-enhanced; DWI, Diffusion-weighted imaging; ^{18}F-PSMA-1007, Fluorine 18-labeled prostate-specific membrane antigen-1007; ISUP, International Society of Urological Pathology; mpMRI, Multiparametric magnetic resonance imaging; NPV, Negative predictive value; PCa, Prostate cancer; PET/MRI, Positron emission tomography/Magnetic resonance imaging; PI-RADS, Prostate imaging reporting and data system; PPV, Positive predictive value; PSA, Prostate-specific antigen; ROC, Receiver-operating characteristic; ROI, Region of interest; SUVmax, Optimal standardized uptake value; TRUS, Transrectal ultrasonography; T1WI, T1-weighted imaging; T2WI, T2-weighted imaging.

* Corresponding author. Department of Medical Imaging, Guangdong Second Provincial General Hospital, Guangzhou, China.
** Corresponding author. Guangzhou Universal Medical Imaging Diagnostic Center, Guangzhou, China.
E-mail addresses: jianggh@gd2h.org.cn (G. Jiang), chenping@uvclinic.cn (P. Chen).

https://doi.org/10.1016/j.prnil.2022.03.003

treatment time and guide the formulation of the best treatment plan.

Multiparametric magnetic resonance imaging (mpMRI), which involves T1-weighted imaging (T1WI), T2-weighted imaging (T2WI), diffusion-weighted imaging (DWI), and dynamic contrast-enhanced (DCE) MRI, has been introduced as a standard for the diagnosis of primary prostate lesions and is useful for guiding prostate biopsy.[4,5] However, the usefulness of DCE MRI in diagnosing PCa is controversial.[6,7] In prostate imaging reporting and data system (PI-RADS), T2WI and DWI are proposed as the dominant sequence for transition zone and peripheral zone lesions. DCE MRI plays a supplementary role when DWI is not sufficient for diagnosis, and DCE positivity only upgrades DWI score three lesions in the peripheral zone to score 4.[8] Considering that DCE MRI does not significantly improve the diagnostic accuracy for PCa but has obvious disadvantages such as being time-consuming and necessitating additional costs, and the potential risk of nephrogenic systemic fibrosis brought by gadolinium contrast reagent, its abandonment has been suggested, and bpMRI has been recommended for more clinical applications.[9–11]

Prostate-specific membrane antigen (PSMA) targeted Positron emission tomography/Magnetic resonance imaging (PET/MRI) is considered to be a promising technology for PCa imaging.[12] The clinical breakthrough of PSMA ligands was achieved with Gallium 68 (^{68}Ga)-labeled PSMA-11, which has been the most commonly used PSMA ligand in clinical trials.[13] However, some limitations for ^{68}Ga-PSMA-11 were gradually exposed in clinical applications, such as requiring an on-site generator to produce with a short half-life, compromised ability to detect smaller lesions with high energy characteristics, and increased PET artifacts surrounding the bladder, due to urethral system excretion.[14,15] With this background, fluorine 18 (^{18}F)-labeled PSMA-1007 has recently received wide attention and has been introduced in clinical practice.[15] Besides its advantages, such as longer half-life, improved resolution of PET image, and higher labeling yields, ^{18}F-PSMA-1007 facilitates non-urinary background clearance superior to that of ^{68}Ga-PSMA-11 through the early hepatobiliary route leading to a reduced bladder background.[16,17] Nevertheless, the clinical reports on ^{18}F-PSMA-1007 PET/MRI are limited. In this study, we evaluate the diagnostic value of ^{18}F-PSMA-1007 PET/MRI and compare it with that of bpMRI for the detection of primary prostate cancer. This study will help promote the clinical applications of ^{18}F-PSMA-1007 PET/MRI and contribute to the literature.

2. Methods

2.1. Study population

Our institution was authorized by the government for the clinical trial research of ^{18}F-PSMA-1007 with financial support. This retrospective study has been approved by the Institutional Ethics Committee (Approved No.2019-01), and written informed consent was obtained from all patients. We initially collected the records of 34 consecutive male patients with suspected PCa preoperatively who underwent ^{18}F-PSMA-1007 PET/MRI and subsequent targeted biopsy for lesions suggestive of PCa between June 2019 and June 2021. Of these patients, 5 were excluded for the following reasons: pathological results were not available for review (n = 2); the patient had other tumors besides PCa (n = 1); the patients had received relevant therapy previously (n = 2). Thus, 29 patients with suspected PCa lesions (n = 48) for targeted biopsy were finally enrolled in our study. Of these lesions, the presence or absence of PCa lesions, tumor Gleason score, and the International Society of Urological Pathology (ISUP) grade for each biopsy specimen were recorded independently according to the 2014 ISUP Modified Grading System.[18,19] Tumor with Gleason score = 3 + 3 and tumor size≥0.5 mL (tumor diameter ≥8 mm), or with Gleason score of ≥7 and tumor diameter≥5 mm was defined as clinically significant PCa.[8,20]

2.2. ^{18}F-PSMA-1007 PET/MRI examination

^{18}F-PSMA-1007 was produced as described by Cardinale et al.[21] with radiochemical purity >95%. The patients were injected with ^{18}F-PSMA-1007 at an injection dosage of 3.7 MBq/kg. After sixty minutes of tracer uptake, a whole-body scan (from the top of the skull to the middle and upper femur, five beds, about 40 min) and subsequent prostate bed fine scan (1 bed, about 15–20 min) were performed after using an integrated PET/MRI system 3T Biograph mMRI (Siemens, Erlangen, Germany). During the prostate bed fine scan, the 3D PET imaging combined with MRI imaging, including transversal T1-weighted imaging, transversal T2-weighted imaging, transversal DWI, sagittal T2-weighted imaging, and coronal T2-weighted imaging, was performed to cover the prostate bed. Apparent diffusion coefficient (ADC) maps of the prostate area were automatically reconstructed from the DWI images acquired using different b-values of 0. 800, and 1400 sec/mm^2. The data acquired from PET and MRI were reconstructed (3D-iterative) using the ordered subset-expectation maximization algorithm (three iterations, 21 subsets, Gaussian postfiltering full width at half maximum 2). The detailed MRI sequence parameters are listed in Supplemental material Table S1.

2.3. Image interpretation

A study coordinator prepared a PowerPoint file showing the ^{18}F-PSMA-1007 PET/MRI images of the lesions targeted for biopsy of each patient prior to the assessments. Two readers board-certified in radiology and nuclear medicine with more than 5 years of experience interpreted the images of each lesion using dedicated software Syngovia version 3.0 (Siemens, Erlangen, Germany) and viewed with reference to the PowerPoint file. Firstly, all bpMRI images of each lesion were interpreted by the two readers blinded to the PET images. Lesions were assigned bpMRI assessment categories of 1–5 according to the simplified PI-RADS v2.1 described by Tamada et al.[20] using only T2WI images and DWI images with ADC maps. The scoring system for T2WI, DWI, and the algorithm for determining bpMRI assessment categories were listed in Supplemental material Tables S2-S3, and a bpMRI assessment category of 3 or higher was characterized as positive. Subsequently, the PET images were evaluated by the two readers with the MRI images as anatomical background and assigned scores of 1–5 for PET according to PSMA-RADS Version 1.0 proposed by Rowe et al.[22] The scoring system was listed in Supplemental material Tables S4. Finally, all lesions were reviewed a second time with access to the individual evaluations of PET and bpMRI images, and a combined PET/MRI interpretation was obtained to determine the final assessment categories by matching the bpMRI assessment categories and PET scores according to the algorithm listed in Supplemental material Tables S5. The PSMA-PET uptake was semi-quantitatively analyzed using the optimal standardized uptake value (SUVmax), which was acquired from the most intense uptake area by drawing a region of interest (ROI). For the ADC values, an ROI was drawn around the lesion on DWI according to the hypointense signal on T2WI. The mean SUVmax and ADC values of a single ROI calculated by the two interpreters were used as observations for analysis and labeled as the SUVmax and ADC of the lesion.

2.4. Biopsy method

All biopsy procedures were performed using the BioJet Fusion Software System (DK Technologies GmbH, Barum, Germany) combined with a transperineal grid transrectal ultrasonography (TRUS) platform (BK Medical, Herlev, Denmark) by an operator who had passed the professional biopsy training. Prior to biopsy, an experienced radiologist was in attendance with targeted lesions marked on MRI and fused to the real-time TRUS images for targeted biopsy. The biopsy core of the target lesion displayed on the fusion image was obtained by biopsy needle (using 18G needles with a sampling length of 17 mm) under TRUS guidance with at least two cores per lesion. During the biopsy, the real-time TRUS images were presented to guarantee the accuracy of needle deployment within the target lesion. The cores were processed for histopathologic analysis by an experienced uropathologist blinded to the imaging results according to the ISUP protocols.

2.5. Statistical Analysis

All statistical analyses were performed using SPSS software version 26.0 (SPSS Inc., Chicago, IL, USA), and MedCalc software version 11.4.2.0 (MedCalc Software Ltd, Ostend, Belgium). The patient clinical characteristics were summarized using descriptive statistics. The continuous variables (ADC) conforming to the normal distribution were represented by the mean ± standard deviation, and the paired sample *t*-test was used to compare those associated with PCa and non-PCa cases. The continuous variables not conforming to the normal distribution (age, PSA, and SUVmax) were represented by the median with interquartile ranges, and the Mann–Whitney *U* test was used to compare those associated with PCa and non-PCa cases. The diagnostic accuracy for ^{18}F-PSMA-1007 PET/MRI and bpMRI were assessed by comparing the imaging findings with the histopathological results as the reference standard using a 2 × 2 contingency table. Their sensitivities, specificities, NPVs, and PPVs were calculated with a 95% Confidence interval (CI), and their AUCs were determined using ROC curves. The ROC curves were used to evaluate the diagnostic accuracies of ADC and SUVmax for detecting PCa and determining their optimal values. The correlations between SUVmax, ADC, and the ISUP grade were analyzed using Spearman's correlation test. $P < 0.05$ was considered significant.

3. Results

3.1. Clinical characteristics of included patients

The clinical characteristics of the included patients are shown in Table 1. According to the histopathological biopsy results, the patients were divided into the PCa group with 22 patients and the non-PCa group with seven patients. The median age and PSA level of the PCa patients were 71 years (range, 63–75 years) and 11.25 ng/mL (range, 8.5–31.6 ng/mL), while those of the non-PCa patients were 65 years (range, 55–67 years) and 7.6 ng/mL (range, 5.2–10.6 ng/mL), respectively. The differences in age and PSA level between the PCa and non-PCa groups showed no statistical significance ($p = 0.199$ and $p = 0.055$, respectively). In 29 patients, 48 suspected PCa lesions were analyzed, which included one lesion in 17 patients, two lesions in eight patients, three lesions in two patients, four lesions in one patient, and five lesions in one patient. Of these 48 lesions, 38 were pathologically confirmed to be clinically significant PCa (6 of ISUP grade 1 with Gleason score 3 + 3, 3 of ISUP grade 2 with Gleason score 3 + 4, 8 of ISUP grade 3 with Gleason score 4 + 3, 8 of ISUP grade 4 with Gleason score 4 + 4, and 13 of ISUP grade 5 with Gleason score 4 + 5/5 + 4/5 + 5, and 10 were non-PCa lesions. Based on the bpMRI, the distribution of the scores for the 38 biopsy-proven PCa lesions were as follows: 3 of PI-RADS score 2, 12 of PI-RADS score 3, 18 of PI-RADS score 4, and 5 of PI-RADS score 5. The distribution of the 10 biopsy-proven non-PCa lesions was as follows: 5 of PI-RADS score 2 and 5 of PI-RADS score 3. Of the 38 biopsy-proven PCa lesions based on the ^{18}F-PSMA PET/MRI, 36 were evaluated as positive and two as negative. All the 10 biopsy-proven non-PCa lesions were labeled as negative. The mean ADC values for the PCa and non-PCa lesions were $(0.7966 \pm 0.15079) \times 10^{-3}$ mm^2/s and $(0.9870 \pm 0.2071) \times 10^{-3}$ mm^2/s, respectively. The median SUVmax values of the PCa and non-PCa lesions were 15.95 (range, 9.7–25.6) and 6.15 (range, 5.2–6.3). The differences between the ADC and SUVmax for the PCa and non-PCa lesions were statistically significant ($p = 0.007$ and $p = 0$, respectively).

3.2. Diagnostic accuracies of bpMRI and ^{18}F-PSMA-1007 PET/MRI for detecting PCa

The results of bpMRI and ^{18}F-PSMA-1007 PET/MRI are summarized in Table 2. Of the 38 lesions with biopsy-proven PCa, 36 were positive, and two were negative based on ^{18}F-PSMA-1007 PET/MRI, while 35 were positive and three were negative based on bpMRI. All of the 10 biopsy-proven non-PCa lesions were negative based on ^{18}F-PSMA-1007 PET/MRI, but only 5 were negative based on bpMRI. The lesion-based sensitivities, specificities, PPV, and NPV of ^{18}F-PSMA-1007 PET/MRI and bpMRI were calculated and are shown in Table 3. Both ^{18}F-PSMA-1007 PET/MRI and bpMRI had relatively high and similar sensitivities (a representative case was shown in Fig. 1) with values of 94.74% (95% CI, 82.25%–99.36%) and 92.11% (95% CI, 78.62%–98.34%), but the specificity, PPV, and NPV of ^{18}F-PSMA-1007 PET/MRI were higher than those of bpMRI as follows: 100% (95% CI, 69.15%–100%) versus 50% (95% CI, 18.71%–81.29%), 100% (95% CI, 90.26%–100%) versus 87.50% (95% CI, 73.20%–95.81%), and 83.33% (95% CI, 51.59%–97.91%) versus 62.5% (95% CI, 24.49%–91.48%), respectively. This may be attributed to the false-positive (a representative case was shown in Fig. 2) and false-negative (a representative case was shown in Fig. 3) on bpMRI compared to ^{18}F-PSMA-1007 PET/MRI. Subsequently, the ROC

Table 1
Clinical characteristics of included patients

Item	PCa*	non-PCa	*P* value
Number of patients	22	7	
Age of patients (year)	71 (63,75)	65 (55,67)	0.199
PSA level of patients (ng/mL)	11.25 (8.5,31.6)	7.6 (5.2,10.6)	0.055
Number of lesions	38	10	
ISUP grade (Gleason score)			
1 (3 + 3)	6 (6)	0	
2 (3 + 4)	3 (3)	0	
3 (4 + 3)	8 (8)	0	
4 (4 + 4)	8 (8)	0	
5 (4 + 5/5 + 4/5 + 5)	13 (9/3/1)	0	
bpMRI PI-RADS score			
1	0	0	
2	3	5	
3	12	5	
4	18	0	
5	5	0	
^{18}F-PSMA PET/MRI assessment category			
Positive (+)	36	0	
Negative (−)	2	10	
ADC of lesions (10^{-3} mm^2/s)	0.7966 ± 0.15079	0.9870 ± 0.2071	0.007
SUVmax of lesions	15.95 (9.7,25.6)	6.15 (5.2,6.3)	0

* All the 38 PCa lesions were defined as clinically significant PCa.

Table 2
Diagnostic test evaluation results of bpMRI and ^{18}F-PSMA-1007 PET/MRI

		Pathologic results		
		PCa	non-PCa	Total
Imaging results	**^{18}F-PSMA-1007 PET/MRI**			
	Positive (+)	36	0	36
	Negative (−)	2	10	12
	Total	38	10	48
	bpMRI			
	Positive (+)	35	5	40
	Negative (−)	3	5	8
	Total	38	10	48

Table 3
Diagnostic accuracy of bpMRI and ^{18}F-PSMA-1007 PET/MRI for detecting PCa

	^{18}F-PSMA-1007 PET/MRI	bpMRI
Sensitivity (95% CI)	94.74% (82.25%–99.36%)	92.11% (78.62%–98.34%)
Specificity (95% CI)	100% (69.15%–100%)	50% (18.71%–81.29%)
PPV (95% CI)	100% (90.26%–100%)	87.50% (73.20%–95.81%)
NPV (95% CI)	83.33% (51.59%–97.91%)	62.50% (24.49%–91.48%)
AUC (95% CI)	0.974 (0.881–0.999)	0.711 (0.562–0.832)
p value	0.0029	

curves for the two imaging examinations for PCa detection were derived, as shown in Fig. 4. The AUC of ^{18}F-PSMA-1007 PET/MRI with the value of 0.974 (95% CI, 0.881–-0.999) was higher than that of bpMRI with the value of 0.711 (95% CI, 0.562–0.832), indicating that ^{18}F-PSMA-1007 PET/MRI have a better diagnostic performance than bpMRI with significance (p = 0.0029).

3.3. ROC curve analyses of SUVmax and ADC for detecting PCa

Since the differences between the ADC and SUVmax for the PCa and non-PCa lesions were statistically significant, their semi-quantitative analyses and optimal cutoffs for detecting PCa were based on the ROC curves shown in Fig. 5. The ROC curve analyses (Table 4) showed that SUVmax had a better diagnostic AUC than ADC (AUC: 0.874 (95% CI, 0.746–0.952) versus 0.776 (95% CI, 0.633–0.884)), but their differences showed no significant meaning ($P = 0.2902$). Specifically, SUVmax demonstrated an 84.21% sensitivity and 100% specificity for the optimal cutoff of 6.7, while ADC showed a 100% sensitivity and 47.37% specificity at 0.79.

3.4. Correlations between SUVmax, ADC, and ISUP grade

The correlations between the SUVmax, ADC, and the ISUP grade are shown in Fig. 6. The ISUP grade was moderately associated with SUVmax (Rho = 0.539, $P = 0$), but not ADC (Rho = −0.105, $P = 0.529$).

4. Discussion

PCa is the second commonly diagnosed cancer in men, and it is predominant in older adults,[1,2] as in our study with a median age of 71 years (range, 63–75 years). For primary PCa, the therapy plan is completely different with different assessments. Radical prostatectomy is the main treatment for early-stage PCa, and is feasible to achieve good therapeutic effects and even cure, while only conservative treatment can be administered to advanced metastatic patients using androgen deprivation therapy or chemotherapy.[23–25] Thus, early detection of PCa is directly related to the patient's treatment plan and prognosis. Since PCa has nonspecific clinical symptoms, early laboratory screening and imaging examinations are important for its detection and diagnosis. Prostate-specific antigen (PSA), a glycoprotein produced by prostate cells, is the commonly used biomarker for screening, and elevated PSA values detected by PSA screening aids in the early diagnosis of PCa.[26,27] However, elevated PSA may also be associated with non-

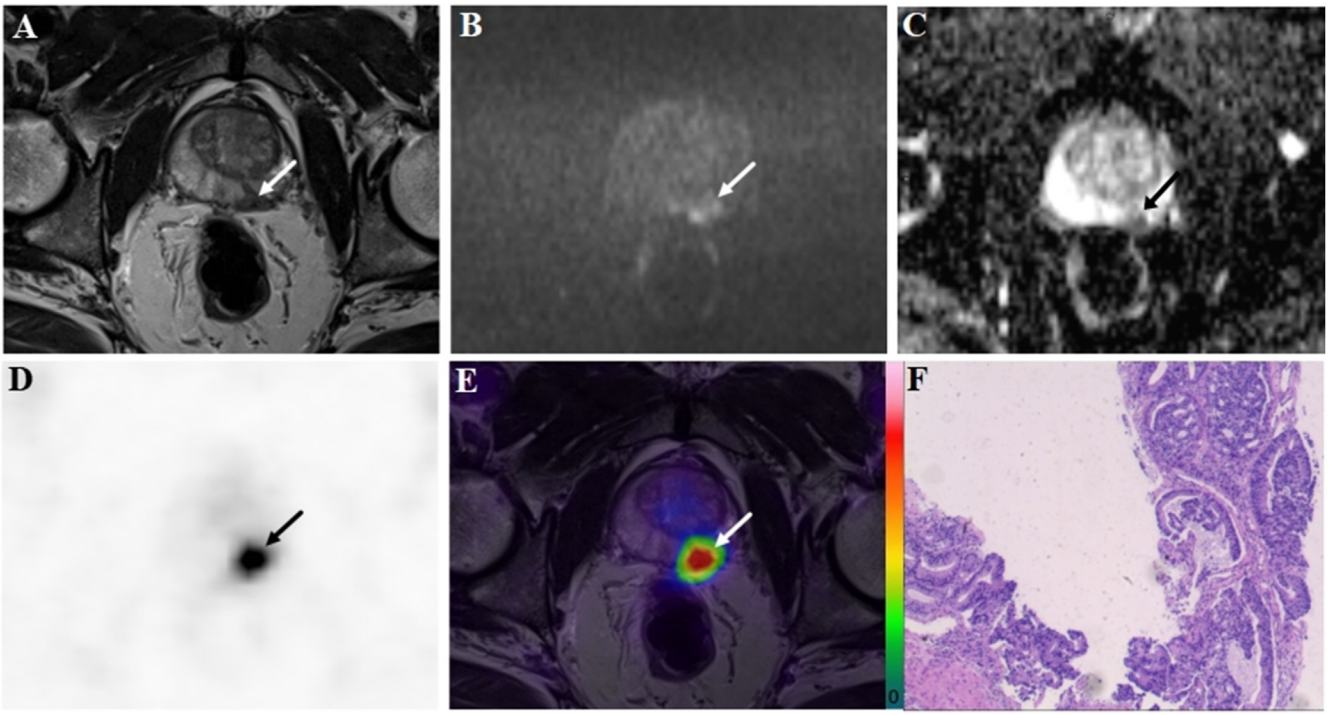

Fig. 1. A 72-year-old patient with a PSA level of 50.8 ng/ml. The lesion with tumor a diameter of 11.7 mm (arrow) was evaluated as positive (PI-RADS score 4) on bpMRI with T2WI image (**A**), DWI image (**B**), and ADC map (**C**), indicating PCa lesion. On the ^{18}F-PSMA-1007 PET image (**D**), the lesion showed an intense uptake with a SUVmax of 79.6 (PSMA-RADS score 5). Combined with bpMRI and PET score, fused ^{18}F-PSMA-1007 PET/MRI image (**E**) further suggested PCa. Subsequent biopsy results (**F**) proved PCa lesion of ISUP grade 5 with Gleason score 5 + 4.

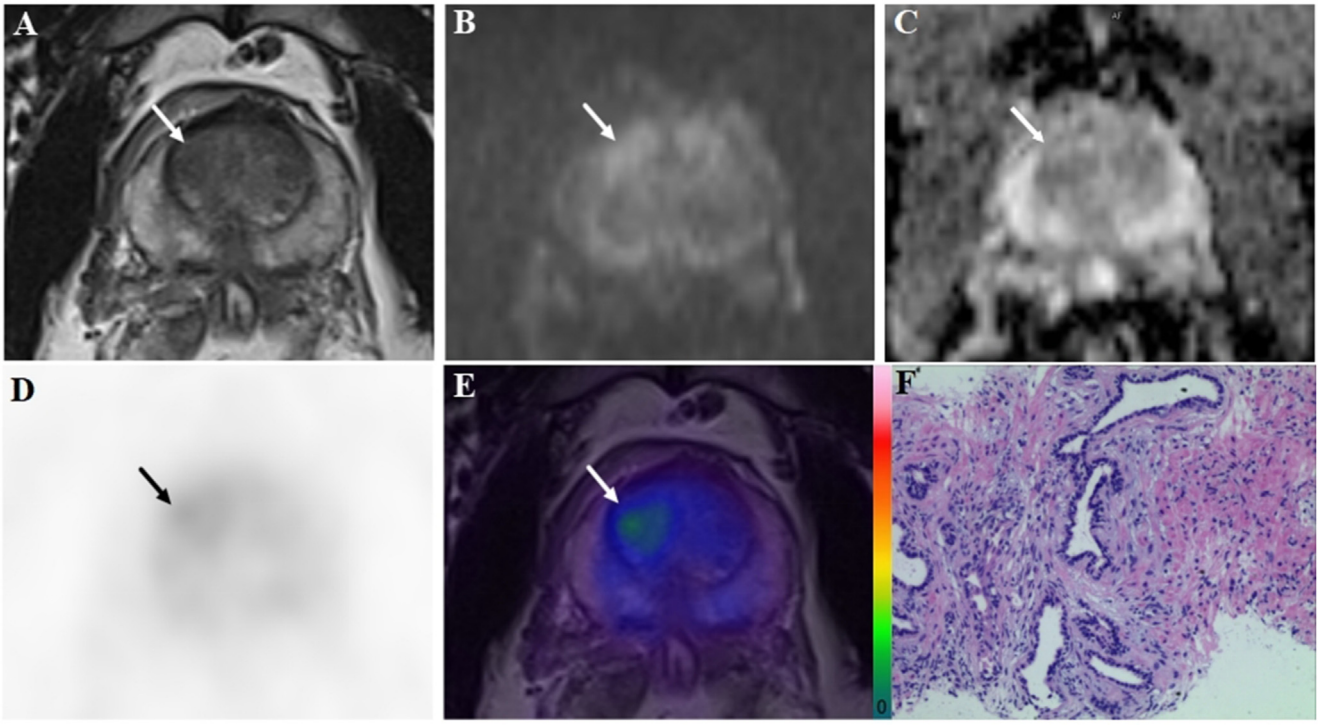

Fig. 2. A 51-year-old patient with a PSA level of 7.1 ng/ml. The lesion (arrow) with a tumor diameter of 13.6 mm was evaluated as positive (PI-RADS score 3) on bpMRI with T2WI image (**A**), DWI image (**B**), and ADC map (**C**), indicating PCa lesion. However, on the ^{18}F-PSMA-1007 PET image (**D**) the lesion showed only a slight uptake with a SUVmax of 3.1 (PSMA-RADS score 2). Combined with bpMRI and PET score, fused ^{18}F-PSMA-1007 PET/MRI image (**E**) suggested benign prostatic lesion, and it was consistent with subsequent biopsy results (**F**).

PCa diseases such as benign prostatic hyperplasia and prostatitis.[28] In agreement with previous reports, our study showed an elevated serum PSA level for both PCa and non-PCa patients, and their differences showed no statistical significance. Thus, for patients with an elevated serum PSA concentration, further imaging is urgently needed to confirm the diagnosis.

The clinical application of mpMRI has become the standard for prostate imaging according to PI-RADS.[6,10] However, bpMRI has gradually been recommended for more clinical applications, given the increase in recent reports,[22,29,30] indicating that it has almost the same diagnostic value as mpMRI in detecting PCa and avoids the disadvantages of mpMRI, including being time-consuming with

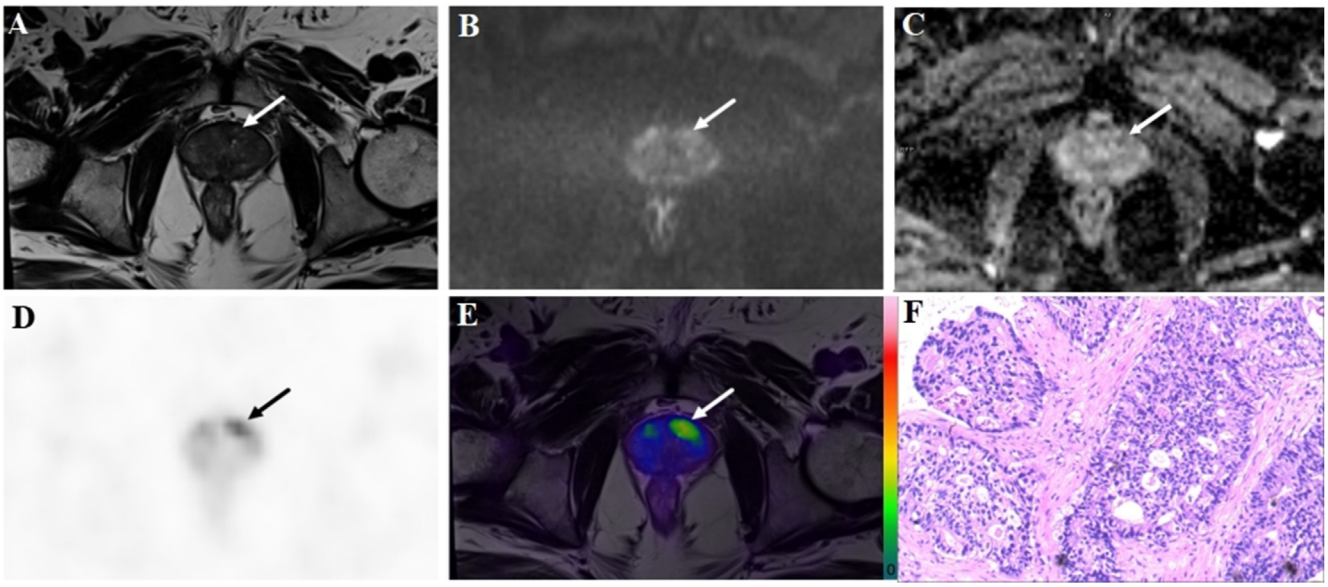

Fig. 3. A 69-year-old patient with a PSA level of 13.5 ng/ml. The lesion (arrow) with a tumor diameter of 10.1 mm was evaluated as negative (PI-RADS score 2) on bpMRI with T2WI image (**A**), DWI image (**B**), and ADC map (**C**), indicating benign lesion. However, on ^{18}F-PSMA-1007 PET image (**D**), the lesion showed an obvious uptake with a SUVmax of 16.2 (PSMA-RADS score 4). Combined with bpMRI and PET score, fused ^{18}F-PSMA-1007 PET/MRI image (**E**) suggested PCa. Subsequent biopsy proved PCa lesion of ISUP grade 4 with Gleason score 4 + 4(**F**).

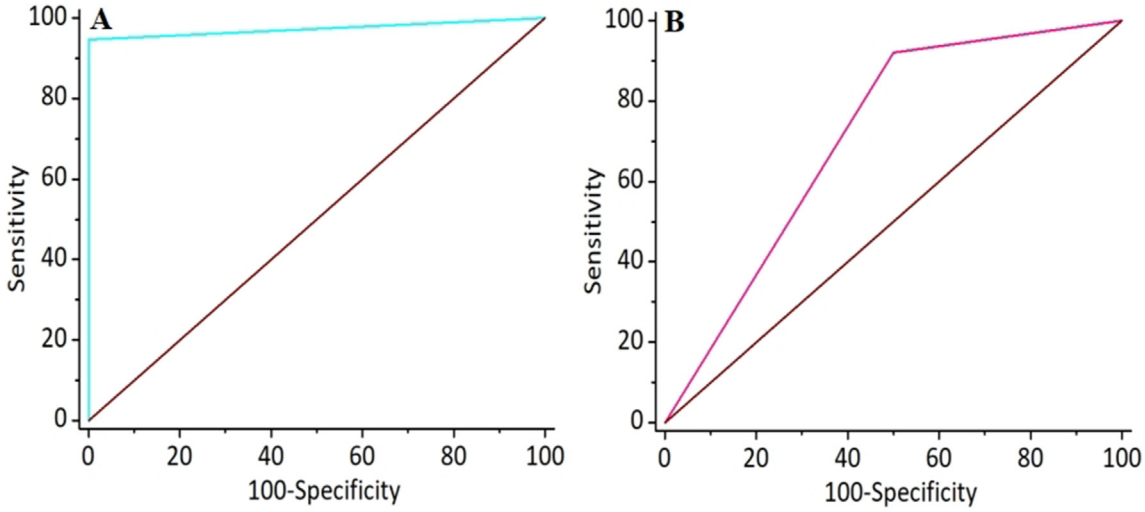

Fig. 4. ROC curves of ^{18}F-PSMA-1007 PET/MRI (**A**) and bpMRI (**B**) for detection of PCa.

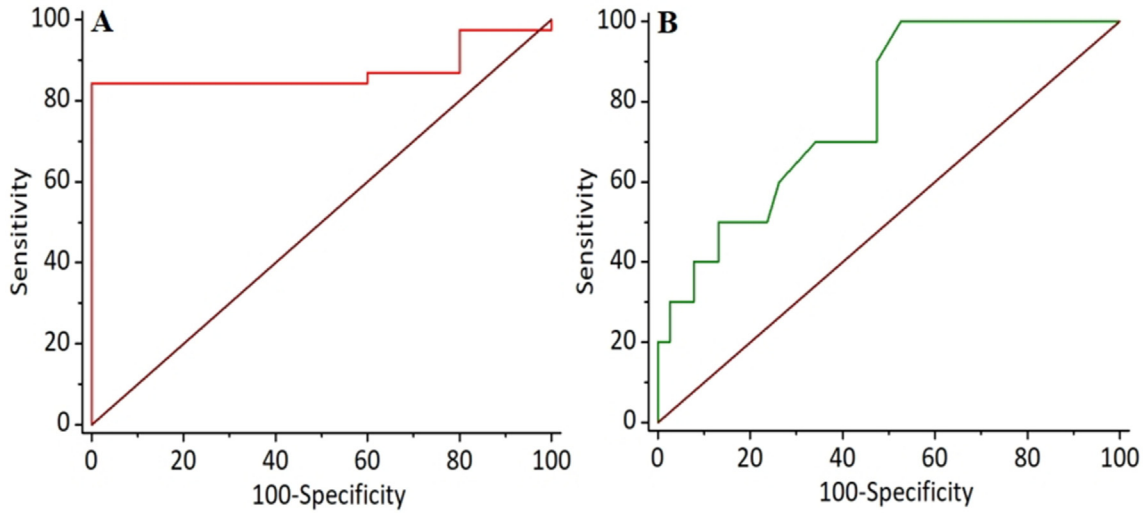

Fig. 5. ROC curve analyses of SUVmax (**A**) and ADC (**B**) for the detection of PCa.

Table 4
Results of the ROC curve analyses

	AUC	optimal cut-off points	Sensitivity	Specificity	95% CI	*P* value
SUVmax	0.874	6.7	84.21%	100.0%	0.746–0.952	0.2902
ADC	0.776	0.79	100.0%	47.37%	0.633–0.884	

additional costs and the potential risk of nephrogenic systemic fibrosis brought by gadolinium contrast reagent.[31] Nevertheless, although mpMRI and bpMRI have been introduced as novel imaging approaches for diagnosis and the localization and characterization of primary prostate lesions and shown to be useful for detecting PCa and guiding prostate biopsy, the problem of relatively low specificity and poor detection of low-grade disease and lower sensitivity within the transitional zone tumors still exists, resulting in missed diagnoses.[32–34] As shown in this study, it also showed that the sensitivity of bpMRI for the detection of PCa reached above 90%, but the specificity was only 50%, resulting in a low AUC of 0.711.

With the development of molecular imaging techniques, PSMA PET was introduced into clinical practice for PCa detection. Different from the anatomical signs obtained from MRI, PSMA PET depicts PCa lesions by detecting the PSMA expression of PCa cells at a molecular level. As PSMA tracer is a transmembrane type II glycoprotein specifically high-expressed in PCa cells with several hundred or thousand more than normal cells and non-PCa cells,[35] PSMA PET exhibits much higher sensitivity and specificity for the detection of PCa than MRI, especially for the detection of occult and small lesions. Among the different PSMA ligands, ^{68}Ga-PSMA-11 is the most used and represents a significant technological breakthrough for clinical applications. However, some disadvantages,

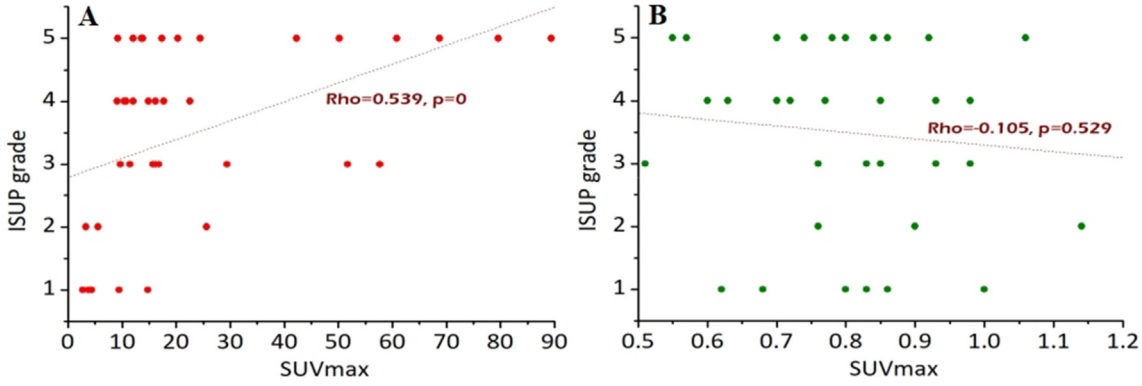

Fig. 6. Correlations between SUVmax (**A**), ADC (**B**), and ISUP grade.

such as shorter half-life, higher energy characteristics, and increased PET artifacts surrounding the bladder, limited its widespread use.[14,15,36] Recent studies have shown that ^{18}F-PSMA-1007, with the same target molecule, made up for these disadvantages. Especially, it was beneficial in overcoming the high background caused by the metabolism of the urethral system during the ^{68}Ga-PSMA-11 process due to the variation in early hepatobiliary metabolism.[15–17] Actually, ^{18}F-PSMA-1007 has been recently introduced to clinical practice after successful preclinical studies.[37–39] To date, most of the recent studies on PCa detection and local staging with ^{18}F-PSMA-1007 were conducted using PET/CT, and the results[40–47] showed that ^{18}F-PSMA-1007 PET/CT were performed with sensitivities ranging from 71% to 100%, specificities ranging from 76% to 100%, and accuracies ranging from 80% to 100%. Although the overall diagnostic value was high, limited by the low resolution of soft tissue on CT, the false-negative and false-positive findings should still be taken into account in some studies, resulting in a relatively low diagnostic accuracy. Promising results in reducing this frequency have been achieved by dual imaging with ^{18}F-PSMA-1007 PET/CT and MRI,[45,47] suggesting that a combination of these two methods will improve the detection of PCa. In recent years, the development of integrated PET/MRI equipment for imaging diagnosis has realized the simultaneous fusion of PET and MRI information, as well as anatomy, function, and metabolism, which may maximize the combined effects of these two technologies.[48–50] In this regard, integrated ^{18}F-PSMA-1007 PET/MRI is expected to show great diagnostic value for PCa imaging. However, the studies on the availability of this method for clinical trials are still limited.[15] Thus, our clinical study was conducted on this premise. Our results confirmed a high diagnostic value of ^{18}F-PSMA-1007 PET/MRI for the detection of PCa lesions with AUC of 0.974, a sensitivity of 94.74%, and a specificity of 100%. Some false-negative and false-positive findings were validly reduced with ^{18}F-PSMA-1007 PET/MRI compared to bpMRI.

The SUVmax value obtained from PET and the ADC value obtained from the DWI component are important semi-quantitative parameters of the lesions, which may reflect lesion characteristics and aggressiveness.[51,52] Their association based on integrated ^{18}F-PSMA-1007 PET/MRI findings is rarely reported. Our study found that the SUVmax and ADC for the PCa and non-PCa lesions showed statistical differences, and they can be used for differential diagnosis. For this reason, we separately studied their ROC curves for diagnosing PCa, and the results showed that SUVmax had a higher diagnostic value over ADC, but there are no significant differences. At their optimal cut-off points, SUVmax and ADC presents a specificity of 100% and sensitivity of 100%, respectively, indicating that a combing of SUVmax and ADC would be beneficial to improving the diagnosis accuracy. Meanwhile, SUVmax value of ^{18}F-PSMA-1007 showed a positive correlation with the ISUP score of the lesion, indicating that ^{18}F-PSMA-1007 overexpression in the PCa cells was associated with a higher ISUP grade, probably resulting in a higher incidence of metastasis and castration resistance.[53] Thus, ^{18}F-PSMA-1007 may be useful for prognostic evaluation and staging of PCa.

Our study had limitations that should be acknowledged. First, ^{18}F-PSMA-1007 PET/MRI is still in the pre-clinical promotion stage, our study was limited by the retrospective, single-center design with a relatively small number of patients. Second, no standardized scoring system is yet available for detecting PCa lesion for the application of bpMRI or ^{18}F-PSMA-1007 PET/MRI in clinical practice. We have formulated a unified algorithms with reference to the literature and strictly implement it to minimize that concern, but further clinical studies are still needed to standardized the scoring system of bpMRI or ^{18}F-PSMA-1007 PET/MRI and confirmed their value. Nevertheless, this study had indicated the high diagnostic value of ^{18}F-PSMA-1007 PET/MRI for the diagnosis of PCa lesions and revealed the associations between the semi-quantitative values of SUVmax and ADC and the ISUP grades for PCa lesions. Our study may provide a reference for the clinical applications of ^{18}F-PSMA-1007 PET/MRI and enrich the literature.

5. Conclusion

^{18}F-PSMA-1007 PET/MRI has a greater diagnostic value for detecting PCa than bpMRI, and SUVmax shows a good correlation with the ISUP grade. For clinical applications, a high SUVmax may indicate a lesion with a high ISUP grade.

Credit Author Statement

Yuping Zeng: Data curation, Methodology, Writing—original draft, Writing—review &editing. **Xiaoming Leng:** Validation, Investigation. **Hengbin Liao:** Resources, Investigation. **Guihua Jiang:** Supervision, Conceptualization, Writing—review and editing. **Ping Chen:** Supervision, Conceptualization, Writing—review and editing.

Conflicts of interest

The authors declare that they have no known competing financial interests or personal relationships that could have appeared to influence the work reported in this paper.

Acknowledgments

The study was supported by the Municipal Health Science and Technology Project of Guangzhou (No.20201A011111 and No.20211A011110) and the Scientific Research Project of Universal Medical Imaging Science and Technology Co., Ltd (UV-2020M06).

Appendix A. Supplementary data

Supplementary data to this article can be found online at https://doi.org/10.1016/j.prnil.2022.03.003.

References

1. Mehdi A, Cheishvili D, Arakelian A, Bismar TA, Szyf M, Rabbani SA. DNA methylation signatures of Prostate Cancer in peripheral T-cells. BMC Cancer 2020;20(1):588. https://doi.org/10.1186/s12885-020-07078-8.
2. Feng RM, Zong YN, Cao SM, Xu RH. Current cancer situation in China: good or bad news from the 2018 Global Cancer Statistics? Cancer Commun 2019;39(1):22. https://doi.org/10.1186/s40880-019-0368-6.
3. Chakravarty D, Huang L, Kahn M, Tewari AK. Immunotherapy for Metastatic Prostate Cancer: Current and Emerging Treatment Options. Urol Clin 2020;47(4):487–510. https://doi.org/10.1016/j.ucl.2020.07.010.
4. Stabile A, Giganti F, Rosenkrantz AB, Taneja SS, Villeirs G, Gill IS, et al. Multiparametric MRI for prostate cancer diagnosis: current status and future directions. Nat Rev Urol 2020;17(1):41–61. https://doi.org/10.1038/s41585-019-0212-4.
5. Drost FH, Osses D, Nieboer D, Bangma CH, Steyerberg EW, Roobol MJ, et al. Prostate Magnetic Resonance Imaging, with or Without Magnetic Resonance Imaging-targeted Biopsy, and Systematic Biopsy for Detecting Prostate Cancer: A Cochrane Systematic Review and Meta-analysis. Eur Urol 2020;77(1):78–94. https://doi.org/10.1016/j.eururo.2019.06.023.
6. Brancato V, Di Costanzo G, Basso L, Tramontano L, Puglia M, Ragozzino A, et al. Assessment of DCE Utility for PCa Diagnosis Using PI-RADS v2.1: Effects on Diagnostic Accuracy and Reproducibility. Diagnostics 2020;10(3):164. https://doi.org/10.3390/diagnostics10030164.
7. Mussi TC, Martins T, Dantas GC, Garcia RG, Filippi RZ, Lemos GC, et al. Comparison between multiparametric MRI with and without post-contrast sequences for clinically significant prostate cancer detection. Int Braz J Urol 2018;44(6):1129–38. https://doi.org/10.1590/S1677-5538.IBJU.2018.0102.
8. Weinreb JC, Barentsz JO, Choyke PL, Cornud F, Haider MA, Macura KJ, et al. PI-RADS Prostate Imaging-Reporting and Data System: 2015, Version 2. Eur Urol 2016;69(1):16–40. https://doi.org/10.1016/j.eururo.2015.08.052.
9. Cho J, Ahn H, Hwang SI, Lee HJ, Choe G, Byun SS, et al. Biparametric versus multiparametric magnetic resonance imaging of the prostate: detection of clinically significant cancer in a perfect match group. Prostate Int 2020;8(4):146–51. https://doi.org/10.1016/j.prnil.2019.12.004.
10. Scialpi M, D'Andrea A, Martorana E, Malaspina C, Aisa MC, Napoletano M, et al. Biparametric MRI of the prostate. Turk J Urol 2017;43(4):401–9. https://doi.org/10.5152/tud.2017.06978.
11. Cai GH, Yang QH, Chen WB, Liu QY, Zeng YR, Zeng YJ. Diagnostic Performance of PI-RADS v2, Proposed Adjusted PI-RADS v2 and Biparametric Magnetic Resonance Imaging for Prostate Cancer Detection: A Preliminary Study. Curr Oncol 2021;28(3):1823–34. https://doi.org/10.3390/curroncol28030169.
12. Grubmüller B, Baltzer P, Hartenbach S, D'Andrea D, Helbich TH, Haug AR, et al. PSMA Ligand PET/MRI for Primary Prostate Cancer: Staging Performance and Clinical Impact. Clin Cancer Res 2018;24(24):6300–7. https://doi.org/10.1158/1078-0432.CCR-18-0768.
13. Kratochwil C, Afshar-Oromieh A, Kopka K, Haberkorn U, Giesel FL. Current Status of Prostate-Specific Membrane Antigen Targeting in Nuclear Medicine: Clinical Translation of Chelator Containing Prostate-Specific Membrane Antigen Ligands into Diagnostics and Therapy for Prostate Cancer. Semin Nucl Med 2016;46(5):405–18. https://doi.org/10.1053/j.semnuclmed.2016.04.004.
14. Afshar-Oromieh A, Haberkorn U, Schlemmer HP, Fenchel M, Eder M, Eisenhut M, et al. Comparison of PET/CT and PET/MRI hybrid systems using a 68Ga-labelled PSMA ligand for the diagnosis of recurrent prostate cancer: initial experience. Eur J Nucl Med Mol Imag 2014;41(5):887–97. https://doi.org/10.1007/s00259-013-2660-z.
15. Awenat S, Piccardo A, Carvoeiras P, Signore G, Giovanella L, Prior JO, et al. Diagnostic Role of ^{18}F-PSMA-1007 PET/CT in Prostate Cancer Staging: A Systematic Review. Diagnostics 2021;11(3):552. https://doi.org/10.3390/diagnostics11030552.
16. Zippel C, Ronski SC, Bohnet-Joschko S, Giesel FL, Kopka K. Current Status of PSMA-Radiotracers for Prostate Cancer: Data Analysis of Prospective Trials Listed on Clinical Trials.gov. Pharmaceuticals 2020;13(1):12. https://doi.org/10.3390/ph13010012.
17. Sengupta S, Krishnan MA, Chattopadhyay S, Chelvam V. Comparison of prostate-specific membrane antigen ligands in clinical translation research for diagnosis of prostate cancer. Cancer Rep 2019;2(4):e1169. https://doi.org/10.1002/cnr2.1169.
18. Epstein JI, Egevad L, Amin MB, Delahunt B, Srigley JR, Humphrey PA. The 2014 International Society of Urological Pathology (ISUP) Consensus Conference on Gleason Grading of Prostatic Carcinoma: Definition of Grading Patterns and Proposal for a New Grading System. Am J Surg Pathol 2016;40(2):244–52. https://doi.org/10.1097/PAS.0000000000000530.
19. Egevad L, Delahunt B, Srigley JR, Samaratunga H. International Society of Urological Pathology (ISUP) grading of prostate cancer-An ISUP consensus on contemporary grading. APMIS 2016;124(6):433–5. https://doi.org/10.1111/apm.12533.
20. Tamada T, Kido A, Yamamoto A, Takeuchi M, Miyaji Y, Moriya T, et al. Comparison of Biparametric and Multiparametric MRI for Clinically Significant Prostate Cancer Detection With PI-RADS Version 2.1. J Magn Reson Imag 2021;53(1):283–91. https://doi.org/10.1002/jmri.27283.
21. Giesel FL, Hadaschik B, Cardinale J, Radtke J, Vinsensia M, Lehnert W, et al. F-18 labelled PSMA-1007: biodistribution, radiation dosimetry and histopathological validation of tumor lesions in prostate cancer patients. Eur J Nucl Med Mol Imag 2017;44(4):678–88. https://doi.org/10.1007/s00259-016-3573-4.
22. Rowe SP, Pienta KJ, Pomper MG, Gorin MA. Proposal for a Structured Reporting System for Prostate-Specific Membrane Antigen-Targeted PET Imaging: PSMA-RADS Version 1.0. J Nucl Med 2018;59(3):479–85. https://doi.org/10.2967/jnumed.117.195255.
23. Teo MY, Rathkopf DE, Kantoff P. Treatment of Advanced Prostate Cancer. Annu Rev Med 2019;70:479–99. https://doi.org/10.1146/annurev-med-051517-011947.
24. Komura K, Sweeney CJ, Inamoto T, Ibuki N, Azuma H, Kantoff PW. Current treatment strategies for advanced prostate cancer. Int J Urol 2018;25(3):220–31. https://doi.org/10.1111/iju.13512.
25. Swami U, McFarland TR, Nussenzveig R, Agarwal N. Advanced Prostate Cancer: Treatment Advances and Future Directions. Trends Cancer 2020;6(8):702–15. https://doi.org/10.1016/j.trecan.2020.04.010.
26. Dunn MW. Prostate Cancer Screening. Semin Oncol Nurs 2017;33(2):156–64. https://doi.org/10.1016/j.soncn.2017.02.003.
27. Chung JS, Morgan TM, Hong SK. Clinical implications of genomic evaluations for prostate cancer risk stratification, screening, and treatment: a narrative review. Prostate Int 2020;8(3):99–106. https://doi.org/10.1016/j.prnil.2020.09.001.
28. Filella X, Foj L. Novel Biomarkers for Prostate Cancer Detection and Prognosis. Adv Exp Med Biol 2018;1095:15–39. https://doi.org/10.1007/978-3-319-95693-0_2.
29. Christophe C, Montagne S, Bourrelier S, Roupret M, Barret E, Rozet F, et al. Prostate cancer local staging using biparametric MRI: assessment and comparison with multiparametric MRI. Eur J Radiol 2020;132:109350. https://doi.org/10.1016/j.ejrad.2020.109350.
30. Woo S, Suh CH, Kim SY, Cho JY, Kim SH, Moon MH. Head-to-Head Comparison Between Biparametric and Multiparametric MRI for the Diagnosis of Prostate Cancer: A Systematic Review and Meta-Analysis. AJR Am J Roentgenol 2018;211(5):W226–41. https://doi.org/10.2214/AJR.18.19880.
31. Junker D, Steinkohl F, Fritz V, Bektic J, Tokas T, Aigner F, et al. Comparison of multiparametric and biparametric MRI of the prostate: are gadolinium-based contrast agents needed for routine examinations? World J Urol 2019;37:691–9. https://doi.org/10.1007/s00345-018-2428-y.
32. Arafa MA, Rabah DM, Khan FK, Farhat KH, Al-Atawi MA. Effectiveness of magnetic resonance imaging-targeted biopsy for detection of prostate cancer in comparison with systematic biopsy in our countries with low prevalence of prostate cancer: our first experience after 3 years. Prostate Int 2021;9(3):140–4. https://doi.org/10.1016/j.prnil.2021.01.001.
33. Greer MD, Choyke PL, Turkbey B. PI-RADS v2: How we do it. J Magn Reson Imag 2017;46:11–23. https://doi.org/10.1002/jmri.25645.
34. Wang X, Bao J, Ping X, Hu C, Hou J, Dong F, et al. The diagnostic value of PI-RADS V1 and V2 using multiparametric MRI in transition zone prostate clinical cancer. Oncol Lett 2018;16:3201–6. https://doi.org/10.3892/ol.2018.9038.
35. Perner S, Hofer MD, Kim R, Shah RB, Li H, Möller P, et al. Prostate-specific membrane antigen expression as a predictor of prostate cancer progression. Hum Pathol 2007;38(5):696–701. https://doi.org/10.1016/j.humpath.2006.11.012.
36. Matushita CS, da Silva AMM, Schuck PN, Bardisserotto M, Piant DB, Pereira JL, et al. 68Ga-Prostate-specific membrane antigen (psma) positron emission tomography (pet) in prostate cancer: a systematic review and meta-analysis. Int Braz J Urol 2021;47(4):705–29. https://doi.org/10.1590/S1677-5538.IBJU.2019.0817.
37. Robu S, Schmidt A, Eiber M, Schottelius M, Günther T, Yousefi BH, et al. Synthesis and preclinical evaluation of novel 18F-labeled Glu-urea-Glu-based PSMA inhibitors for prostate cancer imaging: a comparison with 18F-DCFPyl and 18F-PSMA-1007. EJNMMI Res 2018;8(1):30. https://doi.org/10.1186/s13550-018-0382-8.
38. Cardinale J, Schäfer M, Benešová M, Bauder-Wüst U, Leotta K, Eder M, et al. Preclinical Evaluation of 18F-PSMA-1007, a New Prostate-Specific Membrane Antigen Ligand for Prostate Cancer Imaging. J Nucl Med 2017;58(3):425–31. https://doi.org/10.2967/jnumed.116.181768.
39. Foley RW, Redman SL, Graham RN, Loughborough WW, Little D. Fluorine-18 labelled prostate-specific membrane antigen (PSMA)-1007 positron-emission tomography-computed tomography: normal patterns, pearls, and pitfalls. Clin Radiol 2020;75(12):903–13. https://doi.org/10.1016/j.crad.2020.06.031.
40. Anttinen M, Ettala O, Malaspina S, Jambor I, Sandell M, Kajander S, et al. A Prospective Comparison of 18F-prostate-specific Membrane Antigen-1007

Positron Emission Tomography Computed Tomography, Whole-body 1.5T Magnetic Resonance Imaging with Diffusion-weighted Imaging, and Single-photon Emission Computed Tomography/Computed Tomography with Traditional Imaging in Primary Distant Metastasis Staging of Prostate Cancer (PROSTAGE). Eur Urol. Oncol 2021;4(4):635–44. https://doi.org/10.1016/j.euo.2020.06.012.

41. Giesel FL, Hadaschik B, Cardinale J, Radtke J, Vinsensia M, Lehnert W, et al. F-18 labelled PSMA-1007: biodistribution, radiation dosimetry and histopathological validation of tumor lesions in prostate cancer patients. Eur J Nucl Med Mol Imag 2017;44:678–88. https://doi.org/10.1007/s00259-016-3573-4.
42. Dietlein F, Kobe C, Hohberg M, Zlatopolskiy BD, Krapf P, Endepols H, et al. Intraindividual Comparison of 18F-PSMA-1007 with Renally Excreted PSMA Ligands for PSMA PET Imaging in Patients with Relapsed Prostate Cancer. J Nucl Med 2020;61(5):729–34. https://doi.org/10.2967/jnumed.119.234898.
43. Kuten J, Fahoum I, Savin Z, Shamni O, Gitstein G, Hershkovitz D, et al. Head-to-Head Comparison of 68Ga-PSMA-11 with 18F-PSMA-1007 PET/CT in Staging Prostate Cancer Using Histopathology and Immunohistochemical Analysis as a Reference Standard. J Nucl Med 2020;61(4):527–32. https://doi.org/10.2967/jnumed.119.234187.
44. Sprute K, Kramer V, Koerber SA, Meneses M, Fernandez R, Soza-Ried C, et al. Diagnostic Accuracy of 18F-PSMA-1007 PET/CT Imaging for Lymph Node Staging of Prostate Carcinoma in Primary and Biochemical Recurrence. J Nucl Med 2021;62(2):208–13. https://doi.org/10.2967/jnumed.120.246363.
45. Hong JJ, Liu BL, Wang ZQ, Tang K, Ji XW, Yin WW, et al. The value of 18F-PSMA-1007 PET/CT in identifying non-metastatic high-risk prostate cancer. EJNMMI Res 2020;10:138. https://doi.org/10.1186/s13550-020-00730-1.
46. Kesch C, Vinsensia M, Radtke JP, Schlemmer HP, Heller M, Ellert E, et al. Intraindividual Comparison of 18F-PSMA-1007 PET/CT, Multiparametric MRI, and Radical Prostatectomy Specimens in Patients with Primary Prostate Cancer: A Retrospective, Proof-of-Concept Study. J Nucl Med 2017;58(11):1805–10. https://doi.org/10.2967/jnumed.116.189233.
47. Privé BM, Israël B, Schilham MGM, Muselaers CHJ, Zámecnik P, Mulders PFA, et al. Evaluating F-18-PSMA-1007-PET in primary prostate cancer and comparing it to multi-parametric MRI and histopathology. Prostate Cancer Prostatic Dis 2021;24:423–30. https://doi.org/10.1038/s41391-020-00292-2.
48. Freitag MT, Radtke JP, Hadaschik BA, Kopp-Schneider A, Eder M, Kopka K, et al. Comparison of hybrid (68)Ga-PSMA PET/MRI and (68)Ga-PSMA PET/CT in the evaluation of lymph node and bone metastases of prostate cancer. Eur J Nucl Med Mol Imag 2016;43:70–83. https://doi.org/10.1007/s00259-015-3206-3.
49. Eiber M, Weirich G, Holzapfel K, Souvatzoglou M, Haller B, Rauscher I, et al. Simultaneous 68Ga-PSMA HBED-CC PET/MRI Improves the Localization of Primary Prostate Cancer. Eur Urol 2016;70(5):829–36. https://doi.org/10.1016/j.eururo.2015.12.053.
50. Freitag MT, Radtke JP, Afshar-Oromieh A, Roethke MC, Hadaschik BA, Gleave M, et al. Local recurrence of prostate cancer after radical prostatectomy is at risk to be missed in 68Ga-PSMA-11-PET of PET/CT and PET/MRI: comparison with mpMRI integrated in simultaneous PET/MRI. Eur J Nucl Med Mol Imag 2017;44:776–87. https://doi.org/10.1007/s00259-016-3594-z.
51. Uslu-Beşli L, Bakır B, Asa S, Güner E, Demirdağ Ç, Şahin OE, et al. Correlation of SUVmax and Apparent Diffusion Coefficient Values Detected by Ga-68 PSMA PET/MRI in Primary Prostate Lesions and Their Significance in Lymph Node Metastasis: Preliminary Results of an On-going Study. Mol Imaging Radionucl Ther 2019;28:104–11. https://doi.org/10.4274/mirt.galenos.2019.63825.
52. Zhao J, Mangarova DB, Brangsch J, Kader A, Hamm B, Brenner W, et al. Correlation between Intraprostatic PSMA Uptake and MRI PI-RADS of [68Ga]Ga-PSMA-11 PET/MRI in Patients with Prostate Cancer: Comparison of PI-RADS Version 2.0 and PI-RADS Version 2.1. Cancers 2020;12(12):3523. https://doi.org/10.3390/cancers12123523.
53. Bravaccini S, Puccetti M, Bocchini M, Ravaioli S, Celli M, Scarpi E, et al. PSMA expression: a potential ally for the pathologist in prostate cancer diagnosis. Sci Rep 2018;8:4254. https://doi.org/10.1038/s41598-018-22594-1.